Harmonic Suppression in Capacitor-Run Induction Motors Driven by PWM Choppers Using Evaporation-Based Water Cycle Optimization

N. MURALI, M. ANNAMALAI, S. GOBI MOHAN, R. VIDHYA PRAKASH, S. SADASIVAM
College of Engineering & Technology
University of Technology and Applied Sciences
P.O. Box 477 Postal Code 611 Nizwa
OMAN

Abstract: The speed management is solved by innovative adoptive strategy using optimization algorithm. The formulation of the problem to increase the output voltage is the intended goal. For this, asymmetrical type pulse variation is utilized. By varying the switching instants and use the pulse width modulation to increase power factor. Consequently, an evaporation-based water cycle algorithm with three pulses per quarter cycle is used to construct the reduced cost function. The turn on and turn off angles are simulated and validated with converter topology. According to the data, asymmetrical pulse width modulation performs better than sinusoidal pulse width modulation.

Key-Words: - De-rating, CRIM, Turn off angle, Switching angles, Evaporation operator, PWM

Received: May 27, 2025. Revised: August 5, 2025. Accepted: September 7, 2025. Published: February 4, 2026.

1 Introduction

In the era of new technology, AC chopper used with high efficiency and lesser harmonic distortions for the capacitor-driven induction motor. Low frequency to chop and high frequency to chop are the generalized approaches for controlling AC choppers. The first approach is applied in the literature effectively envisaged for household appliances. The second method is used widely in industries and research. There are different methods available in the literature, sinusoidal PWM, trapezoidal PWM, and selective harmonic elimination technique. The result shows that harmonics eliminated for the SHE method use the RGA-PS algorithm [1]. Resistive and inductive loads are implemented using the conservative type. The filter's design is not provided [2]. The induction motor by phase control operated for different speeds. Due to harmonics, torque pulsation is observed [3-4]. The AC chopper's power factor boost was examined using bee colony optimization. Since passive filters are not utilized for the various switching angles, the harmonic level is higher. [5-8]. The induction motor is controlled by using a field-programmable gate array. The optimal switching angles design by a genetic algorithm [9]. The symmetrical PWM method is investigated for the AC chopper and validated with experimental results [10]. Artificial neural networks and different mathematical formulations [11-12] describe harmonic reduction. The voltage harmonic distortion and simulation-validated result is higher than the standards [13-15]. This article uses an evaporation-based water cycle method to create the optimum high frequency chopping instant for the chopper fed capacitor operated induction motor [16-17]. It solves faster when compared to other traditional optimization techniques [18]. The article arrangement is depicted with different sections. Section 2 designates to AC chopper for step-by-step procedure of obtaining the switching angles. Section 3 explains the results of the proposed algorithm and compares it with the sinusoidal pulse width modulation method. The final section gives a short summary of the article.

2 Problem Formulation

Permanent split capacitor motor structures cage rotor with two windings and static capacitance. Hence it provides rotating magnetic field for self-

starting and excellent enhancement of power quality. This article employs two control strategies: asymmetrical variation of switching moments and sinusoidal variation of switching jiffies. The carrier wave and the triangle wave are compared to get desired switching flashes [21]. Depending on the duty ratio, different pulses are produced. The power circuit consists of two devices in which the main switch for current flow in both directions and the supplementary device for passing the inductive energy to the load. These two switches are complementary and different pulses are used for the switches.

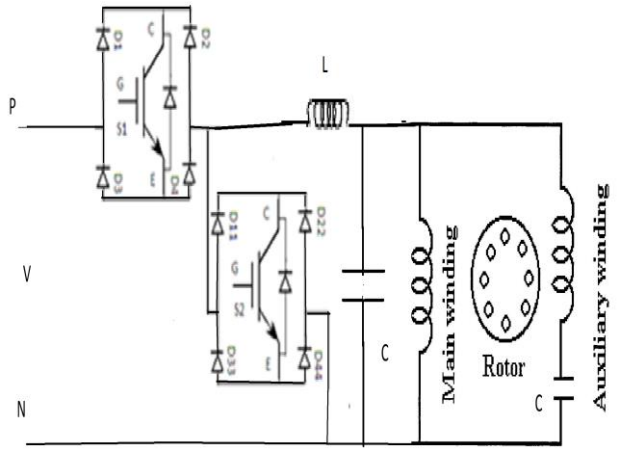

Fig. 1: Induction motor powered by a PWM AC chopper supplied capacitor

An evaporation-based water cycle algorithm is used to design the pulse in asymmetrical pulse width modulation. Enhancement of different metrics mentioned by the mathematical formulations in compliance with the specification of fume extraction. For a sinusoidal waveform with 90 degrees, there are three pulses. N stands for the number of pulses. The device's switching is identified by the letters U1, U2, and U3. W1, W2, and W3 refer to shutting down the gadget. The following is the Fourier series expression for the output voltage.

$$V_o = \sqrt{2}V_i[D_o + \sum_{m=1}^{\infty}(D_n\, Sin(m\omega t) + D_n Cos(m\omega t)] \quad (1)$$

The resultant voltage mentioned below after elimination

$$V_o = \sqrt{2}V_i \sum_{m=1}^{\infty}(D_n\, Sin(m\omega t) \quad (2)$$

Fundamental magnitude D1 articulated [12]

$$D_1 = \frac{1}{\pi}\sum_{r=1}^{P}\left[W_q - U_q - \frac{Sin2W_r - Cos2U_r}{2}\right] \quad (3)$$

Harmonic magnitude Dn articulated

$$D_n = \frac{1}{\pi}\sum_{r=1}^{P}\left[\frac{Sin(m-1)W_r - Sin(m-1)U_r}{n-1} - \frac{Sin(m+1)W_r - Sin(m+1)U_r}{n+1}\right] \quad (4)$$

Overall distortion associated with harmonics is emulated as

$$THD_V = \frac{\sqrt{\sum_{m=3}^{\infty} {V_m}^2}}{V_1} \quad (5)$$

$$THD_i = \frac{\sqrt{\sum_{m=3}^{\infty} I_m^2}}{I_1} \quad (6)$$

Objective function is explained it focus on enhancement of de-rating of the machine by reducing losses.

$$\underset{U,W}{Min}\ H = \sqrt{[(D_1 - V_{set})^2 + D_3^2 + D_5^2 + \cdots D_m^2]} \quad (7)$$

The constraint on a goal function is stated as

$$0 \le U_1 \le W_1 \le \mu \ldots\ldots \le U_q \le W_q \le W_m \quad (8)$$

The on and off switching instants are U and W, where Vset is the reference output voltage. The value of Wmax, or maximum switching angle, is 90 degrees. μ is the borderline established at 30 degrees.

2.1 Algorithm implementation

The mathematical formulation is analogy to the nature inspired real scenario. The recurring process of water flow from the ponds and rivers to the sea is the foundation of this nature inspired algorithm. The starting population of design variables are chosen in the search space, assuming that rainfall occurs at a given place. The stream with the lowest objective function is selected to be the sea. [19]. The remaining stream values flow directly into rivers or the ocean. When rain precipitation start, water goes to the stream as it flows to the sea. Amount of water transferred is influenced by different streams. Rain

water flow to the sea is considered as least cost, which is exchanged on behalf of a precise outcome. In this way, the river and sea are likewise exchanged for the optimum answer. The evaporation operator is used to keep the objective function minimization from converging too quickly. The evaporation process that occurs in the sea creates drizzle in streams and rivers. In order to achieve the optimum results, new river and stream places near the sea are made available by the drizzle. Because of the drizzle, new river and stream locations are created close to the sea to provide the best possible outcome. In order to verify for the minimum objective function for a specific iteration, the stream and river locations are changed. Below is an overview of the algorithm steps. First, determine the search space's starting values [20]. The variables are mentioned in the mathematical formulations. Select random population size for rivers, seas, and streams in step two. Compute the objective function for every stream in step three. Save the random initial population solutions and compute the congregating aloofness for selecting sea besides rivers in fourth pace. Using the governing equations for computing crowding values, determine the flow concentration of rivers and seas in fifth step.

$$Obj_m = GG_m - GG_{Mxy+1}$$

$$m = 1,2,3\ldots, M_{xy} \quad (9)$$

$$NS_m = round\left\{\left|\frac{Obj_m}{\sum_{m=1}^{Msxy} Obj_m}\right| XN_{Stream_s}\right\}$$

$$m = 1,2,3\ldots, M_{xy} \quad (10)$$

The least cost function is determined when the rain water flows to the sea from the streams and marked as fresh site in sixth step as the relevant equation is

$$W_{Stream}^{t+1} = W_{Stream}^{t} + cas * D * (W_{Sea}^{t} - W_{Stream}^{t}) \quad (11)$$

The fresh site streams flow into the rivers and exchange positions of a river with the stream gives the least cost in seventh step as the corresponding equation

$$W_{Stream}^{t+1} = W_{Stream}^{t} + cas * D * (W_{River}^{t} - W_{Stream}^{t}) \quad (12)$$

The fresh spot river drifts into the sea and altercation the positions of the sea with river produces the least cost in eight step given as:

$$W_{River}^{t+1} = W_{River}^{t} + Cas * D * (W_{Sea}^{t} - W_{River}^{t}) \quad (13)$$

The cas represents arbitrary rate [0 -1]. In step nine, the convergence criteria reached, and raining starts. Define new-fangled position with the lowermost rate by figuring the cost. The objective is to eradicate the concentrated values, modernize the least cost and identify lower values in phase ten. Check the convergence requirement after selecting the new sites for the sea and rivers; otherwise, proceed to step six.

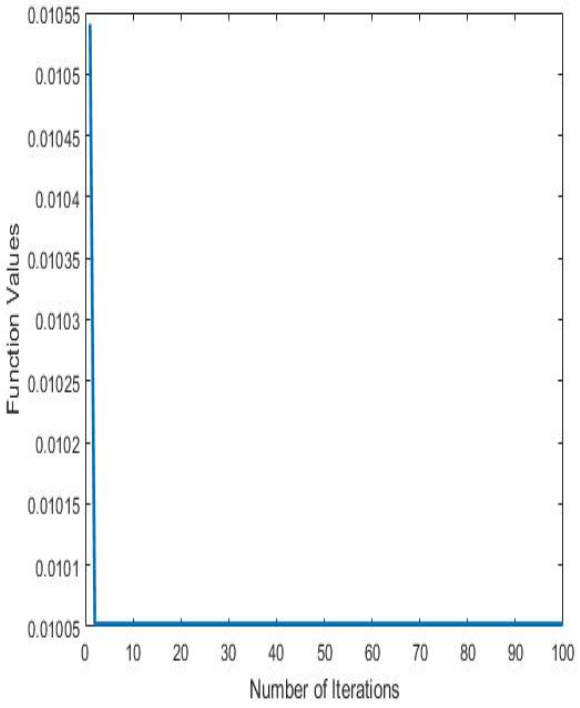

Fig. 2: Convergence graph

Table 1. AWCA on/off angle

V	U1	W1	U2	W2	U3	W3
100	22.00	22.59	31.48	46.00	87.83	90
120	20.00	20.37	45.00	59.49	72.00	90
140	6.00	28.46	30.50	42.00	77.00	90
160	2.48	21.00	35.00	52.65	67.77	90
180	15.13	23.00	46.43	48.00	84.00	90
200	3.00	13.81	35.54	37.00	60.50	90

3 Problem Solution

Tabulation of the optimal switching angle simulated using MATLAB. The suggested approach was contrasted with the literature piece. For the output voltage of 160V, the comparison was tabulated for APWM using an AWCA, APWM using BeCO, and SiPWM. After 100 iterations, the objective function converged.

Table 2. Parameter values of diverse methods

Scheme	%VD	%ID	PF
AWCA	1.05	0.80	0.93
BeCO[11]	16.15	16.15	0.81
SiPWM	21.10	12.90	0.83

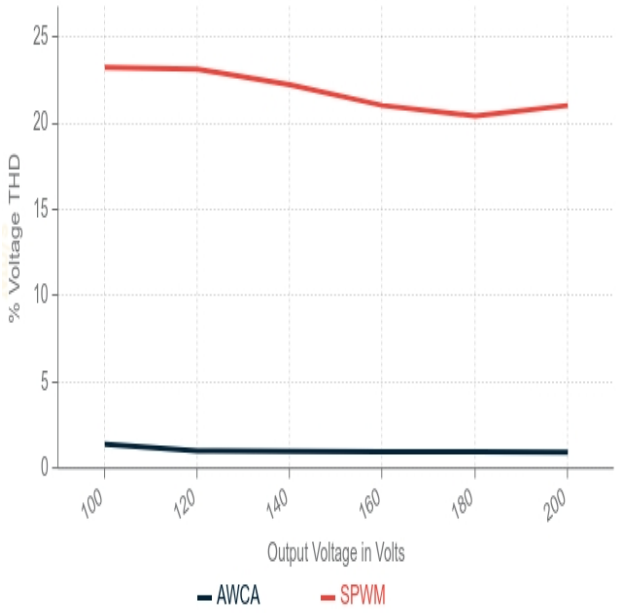

Fig. 3: Discrepancies of %THDv vs voltage

SPWM has a total harmonic distortion voltage of 21.1%, while the asymmetrical technique has 1.02%. The sinusoidal pulse width modulation at 160V results in a 20.05% reduction in the overall harmonic distortion of voltage. It demonstrates that the suggested method's distortion level is lower than the IEEE requirements. Therefore, the speed control works well for under de-rating condition. At 160V, the asymmetrical pulse width modulation has a total harmonic distortions current of 0.59% compared to the technique of sinusoidal pulse width modulation has a 21.1% rate. The overall distortion of harmonics of current is 12.31% less to the sinusoidal pulse width modulation. It concluded that the waveform is sinusoidal due to lesser harmonic distortion.

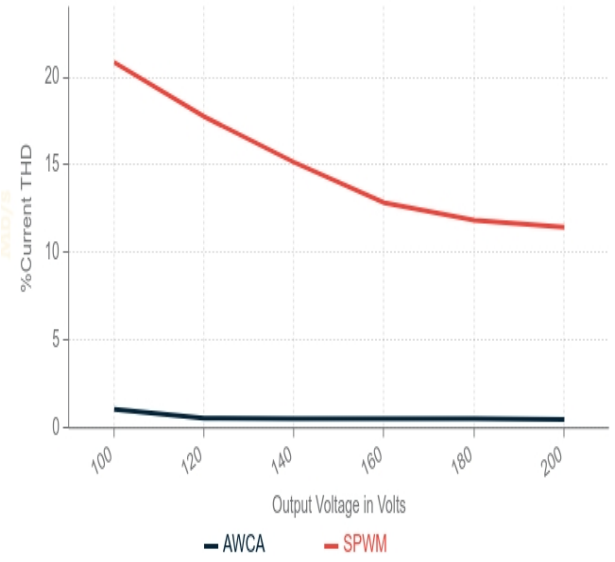

Fig. 4: Discrepancies of %THDi vs voltage

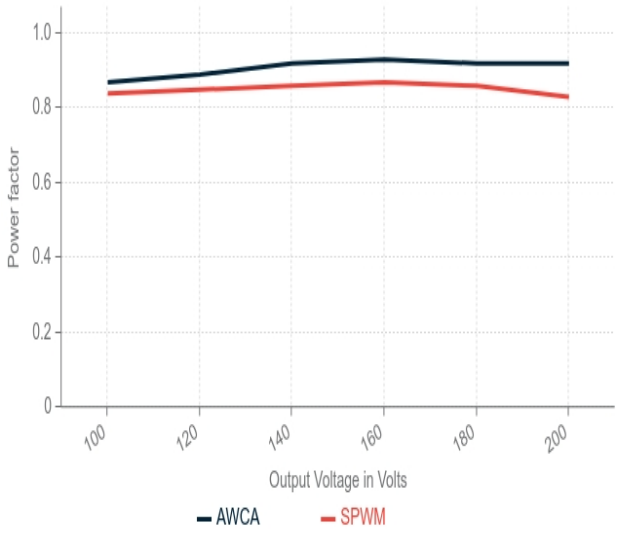

Fig. 5: Discrepancies of Power factor vs voltage

Asymmetrical pulse width modulation is 0.93, while the power factor for sinusoidal pulse width modulation is 0.87. When compared to a sinusoidal pulse with modulation at 160 V, the AC chopper's input power factor is higher. Under various loading scenarios, the enhanced power factor decreases the distortion level in the induction motor. The efficiency of asymmetrical pulse width modulation at 160 V is 71%, while that of sinusoidal pulse width modulation is 53%. When compared to the traditional approach, the efficiency of the asymmetrical pulse width modulation is over 18%. It suggests that there are less losses occurring during operation.

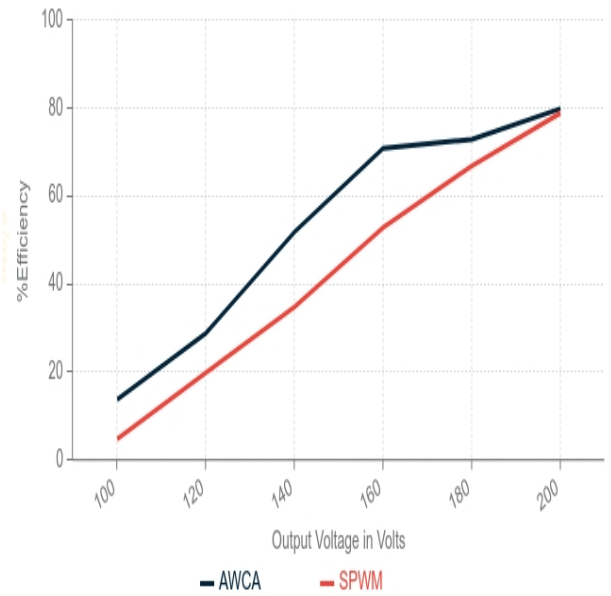

Fig. 5: Discrepancies of Efficiency vs voltage

4 Conclusion

The evaporation water cycle technique is used in this article's selective harmonic elimination method to generate switching angles for the PWM AC chopper. This optimization provides a simple solution for the transcendental equations of the harmonic problem. The simulation result shows that this optimization algorithm reduces the lower-order harmonics of the AC chopper. The output validation is executed by using MATLAB software. The application of this approach to lower harmonics in ac chopper supplied single phase induction motor drives was the focus of further research. drives.

Acknowledgement:
The authors like to thank our HOD of Engineering department & UTAS Management for support.

References:

[1] Z. Shi, L. Wei, J. He, G. Li, and C. Song, "Optimization of Snubber Circuit Parameters for AC–AC Chopper Converter," *Electronics*, Vol. 14, No. 9, pp. 1733-1743, 2025.

[2] B.Zhu , C.Liu , D.Guo, L.Kong, G.Cai , H.Sun,and X.Shao, AC Voltage Synthesis Using Arbitrary Two-Phase Voltages: Frequency, Phase, and Amplitude Modulation for Direct AC–AC Power Conversion, *IEEE Transactions on Power Electronics*, Vol.37, No.10, 2022, pp. 11855-11864.

[3] D.Thomas,et. al, Automatic Voltage Stabilizer using a PWM controlled AC-AC converter topology, *Third International Conference on Intelligent Computing, Instrumentation and Control Technologies* (ICICICT), 2022.

[4] Bounabi , G.Ali, Comparative Analysis of PWM AC Choppers with Different Loads with and Without Neural Network Application, *Wasit Journal of Computer and Mathematics Science*, Vol. 2, No.3, 2023, pp. 16-125.

[5] N.Murali, Annamalai, S.Gobimohan, R.Vidhya Prakash,"Superior Asymmetrical PWM AC Chopper Fed Capacitor Run Induction Motor Drive using Evaporation Based Water Cycle Algorithm," *Communications on Applied Nonlinear Analysis*, Vol.32, No. 6, pp.511-519, 2025.

[6] E. NKOUNA, Arnaud OBONO BIYOBO, P. O. ETOUKE, Y. Paulin, R. Jean, and Serge, "Optimization of DCM Boost Chopper Performance Controlled by Optimal PIDF Regulator for Stand-Alone PV System," *Solar Compass*, pp. 100113–100113, 2025.

[7] M. Bounabi and N. G. Ali, "Comparative Analysis of PWM AC Choppers with Different Loads with and Without Neural Network Application," *Wasit Journal of Computer and Mathematics Science*, Vol. 2, No. 3, pp. 116–125, 2023.

[8] A. M. Nasser, A. Refky, H. Shatla, and A. M. Abdel-hamed, "A grey wolf optimization-based modified SPWM control scheme for a three-phase half bridge cascaded multilevel inverter," *Scientific Reports*, Vol. 14, No. 1, pp. 7016-7026, Mar. 2024.

[9] A. H. Soomro, "Mathematical Modeling and Simulation of AC-AC Three Phase Matrix Converter with LC Filter driving Static Resistive Load," *Quaid-e-Awam University Research Journal of Engineering, Science & Technology*, Vol. 20, No. 2, pp. 116–122, 2022.

[10] A. Udovichenko, E. Grishanov, E. Kosykh, M. Filippov, and M. Dybko, "Single-Level and Two-Level Circuit Solutions for Buck-Boost AC Voltage Regulators with Phase-by-Phase Switches," *Electricity*, Vol. 6, No. 1, pp. 6–16, 2025.

[11] J. Zhu, H. Wu, J. Yang, Y. Wei, J. He, and Y. Xing, "A Family of Dual Power Path Hybrid Converter for AC-AC Power Conversion," *IEEE Transactions on Power Electronics*, Vol. 40, No. 8, pp. 11064–11075, 2025.

[12] N. T. Diep, D. H. Quan, N. H. Minh, and N. K. Trung, "Control Design for Electronic Voltage Stabilizer," *Engineering Technology & Applied Science Research*, Vol. 15, No. 1, pp. 19434–19448, 2025.

[13] Y. Chen, X. Zhang, and S. Yan, "Performance evaluation of grid-forming converters with AC voltage control and reactive power control," *IET conference proceedings*, Vol. 20, No. 32, pp. 288–292, 2025.

[14] M. Faizal, G. Kannayeram, and A. P. Mary, "A novel power quality improved AC voltage controller for soft starting of squirrel cage induction motors," *Journal of Power Electronics*, Vol. 24, No. 7, pp. 1139–1149, 2024.

[15] N. Muhammad, S. Salimin, and A. Abu, "Analysis of Variable Frequency Drive for Induction Motor using Matlab Software," *Journal of Advanced Research in Applied Mechanics*, Vol. 116, No. 1, pp. 117–129, 2024.

[16] N. Ashraf, G. Abbas, Z. Mushtaq, A. U. Rehman, K. Ouahada, and H. Hamam, "Design and implementation of an innovative single-phase direct AC-AC bipolar voltage buck converter with enhanced control topology," *Scientific Reports*, Vol. 14, No. 1, 2024.

[17] W. M. Syed and R. Thakur, Power Factor Improvement and Harmonics Reduction in PWM AC Chopper Fed Three-Phase Induction Motor Drive Using Fuzzy Logic Controller, *IEEE Delhi Section Conference (DELCON), New Delhi, India*, 2022, pp. 1-6.

[18] Murali, N., Balaji, V, Enhanced Asymmetrical PWM AC chopper fed capacitor run induction motor drive using Bacterial Foraging Optimization Algorithm. *IEEE conference*, 2018, pp. 3457-3462.

[19] R. I. Jabbar, Saad Mekhilef, Marizan Mubin, Obaid Alshammari, and A. Kazaili, "A Fast MPPT Method Based on Improved Water Cycle Optimization Algorithm for Photovoltaic Systems under Partial Shading Conditions and Load Variations," *IEEE Open Journal of the Industrial Electronics Society*, pp. 1–16, 2024.

[20] Hajar Alimorad, "Optimization of dynamic control systems using water cycle algorithm," *Journal of the Franklin Institute*, Vol. 361, No. 8, pp. 106831–106831, 2024.

[21] A. Abbou, T. Nasser, H. Mahmoudi, M. Akherraz, A. Essadki," Induction Motor controls and Implementation using dSPACE", *WSEAS Transactions on Systems and Control*, Volume 7, pp. 26-35, 2012